Mater. Res. Soc. Symp. Proc. Vol. 1071 © 2008 Materials Research Society 1071-F07-08

Nonvolatile resistive switching characteristics of HfO_2 with Cu doping

Weihua Guan[1], Shibing Long[1], Ming Liu[1], and Wei Wang[2]
[1]Lab of Nano-fabrication and Novel Devices Integrated Technology, Institute of Microelectronics, Chinese Academy of Sciences, Beijing, 100029, China, People's Republic of
[2]College of Nanoscale Science and Engineering, University at Albany, Albany, NY, 12203

ABSTRACT

In this work, resistive switching characteristics of hafnium oxide (HfO_2) with Cu doping prepared by electron beam evaporation are investigated for nonvolatile memory applications. The top metal electrode/ hafnium oxide doped with Cu/n^+ Si structure shows two distinct resistance states (high-resistance and low-resistance) in DC sweep mode. By applying a proper bias, resistance switching from one state to the other state can be achieved. Though the ratio of high/low resistance is less than an order, the switching behavior is very stable and uniform with nearly 100% device yield. No data loss is found upon continuous readout for more than 10^4 s. The role of the intentionally introduced Cu impurities in the resistive switching behavior is investigated. HfO_2 films with Cu doping are promising to be used in the nonvolatile resistive switching memory devices.

INTRODUCTION

Recently, reversible and reproducible resistive switching phenomena induced by external electric field have been extensively studied due to its potential applications in resistive random access memories (RRAM) [1]-[14]. The typical cell of this kind of memory is a capacitor-like structure: a functional material sandwiched between two conductive electrodes. This type of memory devices can be characterized by two distinct resistance states: OFF state (with high resistance) and ON state (with low resistance). RRAM offers the possibility of high density integration, low power operation, and multilevel storage. The current candidate materials for this type of memories include ferromagnetic material such as $Pr_{1-x}Ca_xMnO_3$ (PCMO) [1], doped perovskite oxide such as $SrZrO_3$ [2] and $SrTiO_3$ [3], organic materials [4], and binary metal oxides such as NiO [5], TiO_2 [6], ZrO_2 [7], Cu_xO [8], and even doped SiO_2 [9]. Among all these candidates, binary transition metal oxides excel the others due to their simple structure, easy fabrication process and compatibility with the complementary metal-oxide semiconductor (CMOS) technology [10]. Although HfO_2 films are considered to be the promising gate dielectric in advanced CMOS devices, its resistive switching behavior is not fully explored, except for its unipolar switching behavior [11]-[12], i.e., turning ON and OFF occurs with the same voltage polarity. In our previous work [13], we studied the resistive switching characteristics of zirconium oxide embedded with ultrathin Au layer (with Au doping) and demonstrated that the intentionally introduced Au in ZrO_2 films can significantly improve the device yield. Au atoms, unfortunately, may be fatal for the integration with CMOS devices.

In this work, we report the bipolar resistive switching characteristics of HfO_2 with Cu doping for nonvolatile memory applications. Cu is nowadays emerging as an alternative to Al for metallization patterns, particularly for interconnect system having smaller dimensions and thus is friendly with CMOS technology. The top Au electrode/ HfO_2 doped with Cu/n^+ Si bottom electrode structure is fabricated and electrically characterized. The fabricated devices show excellent uniformity and stability. The possible mechanism for resistive switching is also investigated.

EXPERIMENT DETAILS

A heavily doped (ρ~3.5×10^{-3} Ω·cm) n-type Si substrate is used as the bottom electrode. After chemically cleaning this n^+ silicon substrate, three sequential layers of HfO_2/Cu/HfO_2 (with thickness of 30/2/30 nm respectively) are deposited on the substrate via e-beam evaporation. The deposition ramp for the thin Cu layer and the HfO_2 layer is 0.2 Å/s and 0.9 Å/s, respectively. The chamber pressure is around 1.1×10^{-6} Torr. The thickness of each layer is monitored by a quartz crystal oscillator. Post-deposition annealing at 600 ºC is carried out in N_2 ambient (3 L/min) to thermally diffuse the Cu atoms into HfO_2 matrix. Finally, 50 nm-thick square-shaped Au top electrodes are evaporated and defined by the lift-off process to form areas ranging from 0.36 mm^2 to 1 mm^2. For the purpose of comparison, control samples without Cu doping in HfO_2 films are simultaneously fabricated with the same process and parameter. The current-voltage (*I-V*) characteristics of the fabricated devices are analyzed by Keithley 4200 semiconductor characterization system in double-sweep mode, voltage list mode and sampling mode. All the measurements were performed at room temperature and under atmosphere condition. The bias voltage is applied on the top electrode with the n^+ Si bottom electrode grounded.

RESULT AND DISCUSSION

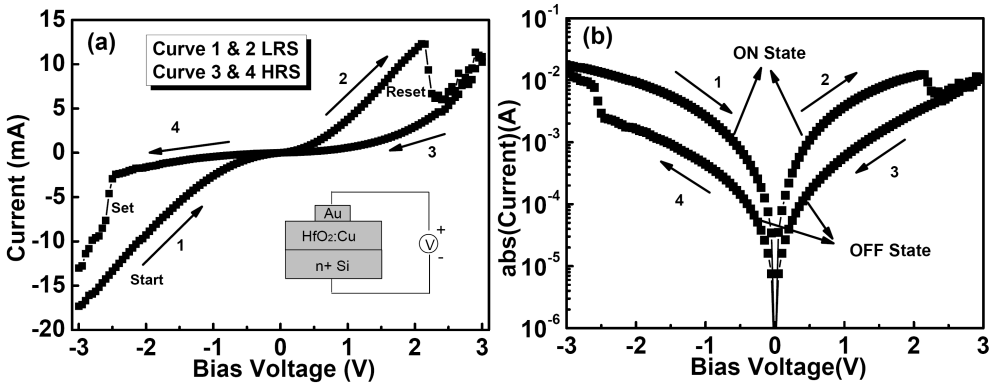

Figure 1. Typical I-V characteristics of devices with area of 0.49 mm^2 in (a) linear scale and (b) semi-log scale. The voltage is swept in the direction as follows: -3 V→0 V→3 V→0 V→-3 V, as indicated by the arrows. Inset of the upper window shows the schematic test configuration.

Figure 1 (a) shows a typical *I–V* curve measured by two terminal top-bottom electrodes (as illustrated in the inset of Figure 1 (a)) in linear scale. Figure 1(b) replots the same curve in semi-logarithmic scale. The voltage loop is swept as follows: $-V_{max}\rightarrow0V\rightarrow+V_{max}\rightarrow0V\rightarrow-V_{max}$. Hysteresis of *I-V* curve is clearly observed when the bias is swept back and forth, which

indicates the existence of different resistance states. Here, we define low resistance state (LRS) and high resistance state (HRS) for upper and lower branches of the *I–V* curve, respectively. As shown in Figure 1, resistive switching from LRS (or ON state) to HRS (or OFF state) is induced by increasing the voltage up to a positive value (e.g. 2.3 V) where a decrease in current is observed. During this process, the negative differential resistance (NDR) behavior is clearly observed. The current of the OFF state increases with increasing the voltage bias in the negative direction and a switching from OFF state to ON state can be achieved at a negative bias voltage (e.g. -2.6 V). The reversible transitions between ON and OFF state can be traced for a large number of times. At a proper reading voltage (e.g. 0.3 V), the resistance of LRS and HRS can be extracted.

There are several points worthy mentioning about the *I-V* curve observed. First, there is no need of electroforming process for our Cu doped HfO_2 films, which is a required step by many others [5]-[7]. This is a superior property for real application. The possible reasons will be discussed in the following discussion. Second, resistive switching from LRS to HRS (turning OFF) occurs only when positive bias is applied and vice versa. This is known as the bipolar switching behavior, which means the switching is polarity dependent. This characteristic is different from the unipolar switching reported by Park *et al.* [11] and Lee *et al.* [12] with an undoped HfO_2 films. The last point is that the resistance ratio between HRS and LRS at a reading voltage (e.g. 0.3 V) is less than an order (approximately six), smaller than many other structures [2]-[6], but comparable to the BST thin films reported by Oligschlaeger *et al.* [14]. Despite its small signal margin for sensing different resistance states, the device yield is nearly 100%. For the total number of 1000 devices fabricated, almost every device under test shows the same reproducible switching behavior. This is consistent with the conclusion of our previous study of Au doped ZrO_2 films [13]: doping in the oxide can improve the device yield due to the more uniform and homogeneous trap concentrations. In the contrary, the control samples without Cu doping show unstable and noisy switching behaviors.

In order to evaluate the potential of our doped devices for application in nonvolatile memories, tests concerning reliability issues are performed. The repeatable resistive switching characteristic is measured in voltage list sweep mode by performing a series of consecutive write-read-erase-read (W/R/E/R) cycles. The amplitude of the write/erase voltage is ±3 V and of readout voltage is +0.3 V. As shown in Figure 2, although there is a variation of resistance values in both LRS and HRS, more than one hundred times of W/R/E/R cycles without serious sensing window deterioration are demonstrated.

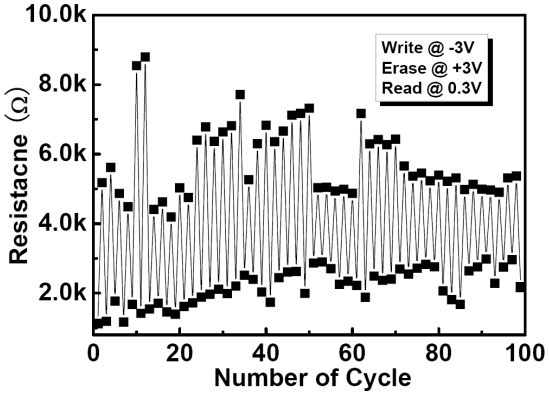

Figure 2. Endurance performance of the fabricated devices.

Figure 3 shows the capability of the devices to retain both resistance states. During this measurement, the device is first turned ON or OFF by applying -3 V or +3 V stress for a short time and then a continuous readout voltage (+0.3 V) is applied. The test scheme is briefly sketched in the inset of Figure 3. The read voltage samplings the resistance value of the device every 60 seconds. As shown in Figure 3, the resistance values of both LRS and HRS are stable and show no detectable sign of degradation over 10^4 s, confirming the nonvolatile nature and the non-destructive readout property of the devices.

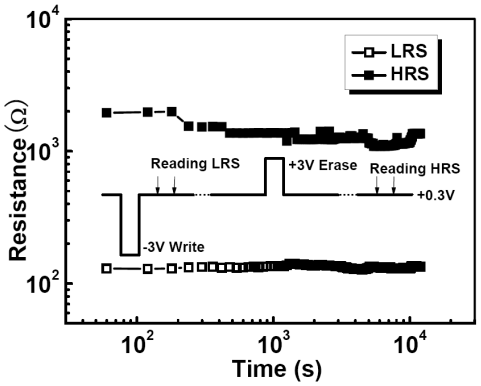

Figure 3. The nonvolatility performance of the fabricated devices.

By far, the physical origins of the resistive switching phenomena are still in debate. Hypothetical models, attempting to explain the resistive switching phenomena, can be divided into two main categories: one is the interface effect and the other is the bulk effect. As for the interface effect, Sawa *et al.* proposed a model of the alternation of Schottky barrier by carriers trapping/detrapping at the interface, causing the resistance changed [1,3]. For the bulk effect, Simmons and Verderber (SV model) proposed a model based on the conductivity modulation by charge trapping 40 years ago [15], and this model is also adopted to account for the organic memory devices [16]. Moreover, several classic conduction mechanisms in insulated materials have also been proposed, such as space charge limited current (SCLC) [8], Frenkel-Pool (F-P) emission, forming and rupture of metallic filaments (ohmic) [6] or a combination of them [2].

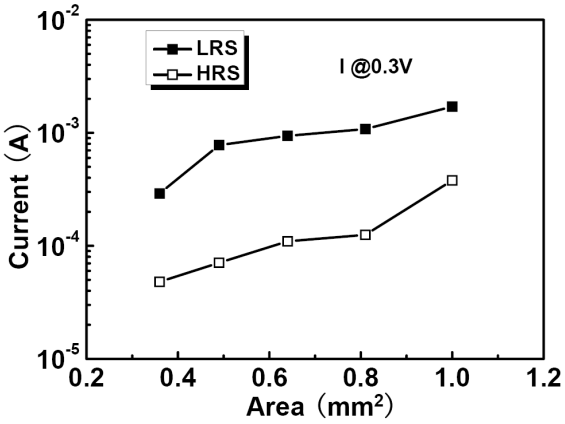

Figure 4. The current dependence on electrode area for both LRS and HRS.

According to the observed *I-V* characteristics of our devices, the interface effect can be firstly ruled out due to the different switching performance between doped and undoped samples, which have the same interface (fabricated under the same condition). While for the classic conduction mechanisms mentioned above, they can be distinguished through the isothermal *I-V* correlation [17]: linear *I*~*V* for ohmic, ln *I* /*V*~$V^{1/2}$ for F-P conduction, and I~V^2 for SCLC. According to our *I-V* fitting results, the ohmic and the F-P conduction can be excluded. The movement of Cu ions for the switching mechanism is not possible since the *I-V* correlation of ion conduction is linear. The impossibility of filament conduction (ohmic) is further confirmed by the measurement of the current as a function of the contact areas. As shown in Figure 4, the current of both LRS and HRS shows obvious area dependence, contrary to the localized filamentary conduction that has an independent current of the area. As for SCLC condution, *I-V* loop should be anticlockwise in the positive voltage range [8], while the *I-V* curve of our devices shows a clockwise behavior, as shown in Figure 1. Therefore, SCLC mechanism may not be responsible in our devices with a unique doping structure.

The experimental features of the *I-V* characteristics, interestingly, are identical to those described by SV model [15]: N-shaped *I–V* characteristic and clockwise switching in the positive voltage range. Moreover, due to the homogeneous conduction of SV model, the dependence of current on electrode area is also expected. More over, the polarity dependence of switching can be understood by SV model as follows: when electrons are injected and trapped in HfO_2 by applying a positive voltage (e.g., V_{reset}), an interior electric field is built, resulting in the decrease of the conductivity, which corresponds to the reset process. When a negative voltage (e.g., V_{set}) is applied, electrons are ejected out. As a result, the conductivity increases, corresponding to the set process. SV model involves carrier transportation through defects, which act as charge trapping sites. SV's description of these trapping sites is deep-level Au atoms provided by the electroforming process, which moves metal atoms from the electrode into the functional layer where they form an impurity band of charge transport levels [15]. Since we deliberately diffuse the Cu atoms into HfO_2 matrix during the fabrication process, the electroforming process can be exempted, as observed in the experiment. Similar phenomena of the initial low resistance state and forming-free property are also found in other doped materials [2]-[3], [18]-[19]. Due to the excellent phenomenal fitting and self-consistent explanation with SV model, we infer that the dominant mechanism for our devices may be the conductivity modulation by charge transportation in impurity band provided by Cu doping.

CONCLUSIONS

In summary, the top Au electrode/HfO_2 with copper doping/n^+ Si sandwich structure is fabricated and investigated for the nonvolatile memory applications. The intentionally introduced Cu impurities, acting as the electron traps, not only provide an effective way to improve the device yield, but also exempt the necessary of electroforming process. All the electrical observations fit the perditions of SV model quite well. The fabrication process is simple and compatible with current CMOS technology. The fabricated devices possess the properties of reversible and reproducible resistive switching, nondestructive readout, good cycling performance and nonvolatility. These excellent reliability performances indicate that Cu doped HfO_2 film is highly promising in the application for future nonvolatile resistive switching memory device.

ACKNOWLEDGMENTS

This work was supported by the Hi-Tech Research and Development Program of China (863 Program) under Grant No 2008AA031403, the National Basic Research Program of China (973 Program) under Grant No 2006CB302706 and the National Natural Science Foundation of China under Grant Nos 90607022 and 60506005.

REFERENCES

1. A. Sawa, T. Fujii, M. Kawasaki, and Y. Tokura, Appl. Phys. Lett., **85**, 4073 (2004).
2. C.-C. Lin, B.-C. Tu, C.-C. Lin, C.-H. Lin, and T.-Y. Tseng, IEEE Electron Device Lett., **27**, 725 (2006).
3. T. Fujii, M. Kawasaki, A. Sawa, H. Akoh, Y. Kawazoe, and Y. Tokura, Appl. Phys. Lett., **86**, 012107 (2004).
4. Y. Song, Q. D. Ling, S. L. Lim, E. Y. H. Teo, Y. P. Tan, L. Li, E. T. Kang, D. S. H. Chan, and C. Zhu, IEEE Electron Device Lett., **28**, 107 (2007).
5. J.-W. Park, J.-W. Park, K. Jung, M. K. Yang, and J.-K. Lee, J. Vac. Sci. Technol. B, **24**, 2205 (2006).
6. B. J. Choi et al., J. Appl. Phys., **98**, 033715 (2005).
7. D. Lee, H. Choi, H. Sim, D. Choi, H. Hwang, M.-J. Lee, S.-A. Seo, and I. K. Yoo, IEEE Electron Device Lett., **26**, 719 (2005).
8. A. Chen, S. Haddad, Y. C. Wu, Z. Lan, T. N. Fang, and S. Kaza, Appl. Phys. Lett., **91**, 123517 (2007).
9. C. Schindler, S. C. P. Thermadam, R. Waser, and M. N. Kozicki, IEEE Trans. Electron Devices, **54**, 2762 (2007).
10. 1. G. Baek et al., in *IEDM Tech. Dig.*, 587 (2004).
11. I.-S. Park, K.-R. Kim, S. Lee, and J. Ahn, Jpn. J. Appl. Phys., **46**, 2172 (2007).
12. H.-Y. Lee, P.-S. Chen, C.-C. Wang, S. Maikap, P.-J. Tzeng, C.-H. Lin, L.-S. Lee, and M.-J. Tsai, Jpn. J. Appl. Phys., **46**, 2175 (2007).
13. W. Guan, S. Long, R. Jia, and M. Liu, Appl. Phys. Lett., **91**, 062111 (2007).
14. R. Oligschlaeger, R. Waser, R. Meyer, S. Karthäuser, and R. Dittmann, Appl. Phys. Lett., **88**, 042901 (2006).
15. J. G. Simmons and R. R. Verderber, Proc. R. Soc. Lond. A, Math. Phys. Sci., **301**, 77 (1967).
16. L. D. Bozano, B. W. Kean, V. R. Deline, J. R. Salem, and J. C. Scott, Appl. Phys. Lett., **84**, 607 (2004).
17. S. M. Sze, Physics of Semiconductor Device, 2nd ed. New York: Wiley, 1981.
18. M. Villafuerte, S. P. Heluani, G. Juárez, G. Simonelli, G. Braunstein, and S. Duhalde, Appl. Phys. Lett., **90**, 052105 (2007).
19. D. Lee, D. Seong, I. Jo, F. Xiang, R. Dong, S. Oh, and H. Hwang, Appl. Phys. Lett., **90**, 122104 (2007).